ISTITUTO NAZIONALE DI FISICA NUCLEARE – ISTITUTO NAZIONALE DI FISICA NUCLEARE - ISTITUTO NAZIONALE DI FISICA NUCLEARE - ISTITUTO NAZIONALE DI FISICA NUCLEARE - ISTITUTO NAZIONALE DI FISICA NUCLEARE - ISTITUTO NAZIONALE DI FISICA NUCLEARE - ISTITUTO NAZIONALE DI

# Laboratori Nazionali di Frascati

Submitted to Nucl. Instr. & Meth. in Phys. Res. A

LNF-92/107 (P)
16 Dicembre 1992

M. Castellano, N. Cavallo, F. Cevenini, S. Kulinski, P. Patteri, F. Tazzioli, M. Vescovi:

## COMMISSIONING AND PERFORMANCE OF A LOW EMITTANCE, LONG PULSE ELECTRON GUN FOR THE SC LINAC LISA

PACS.: 29.15.Dt

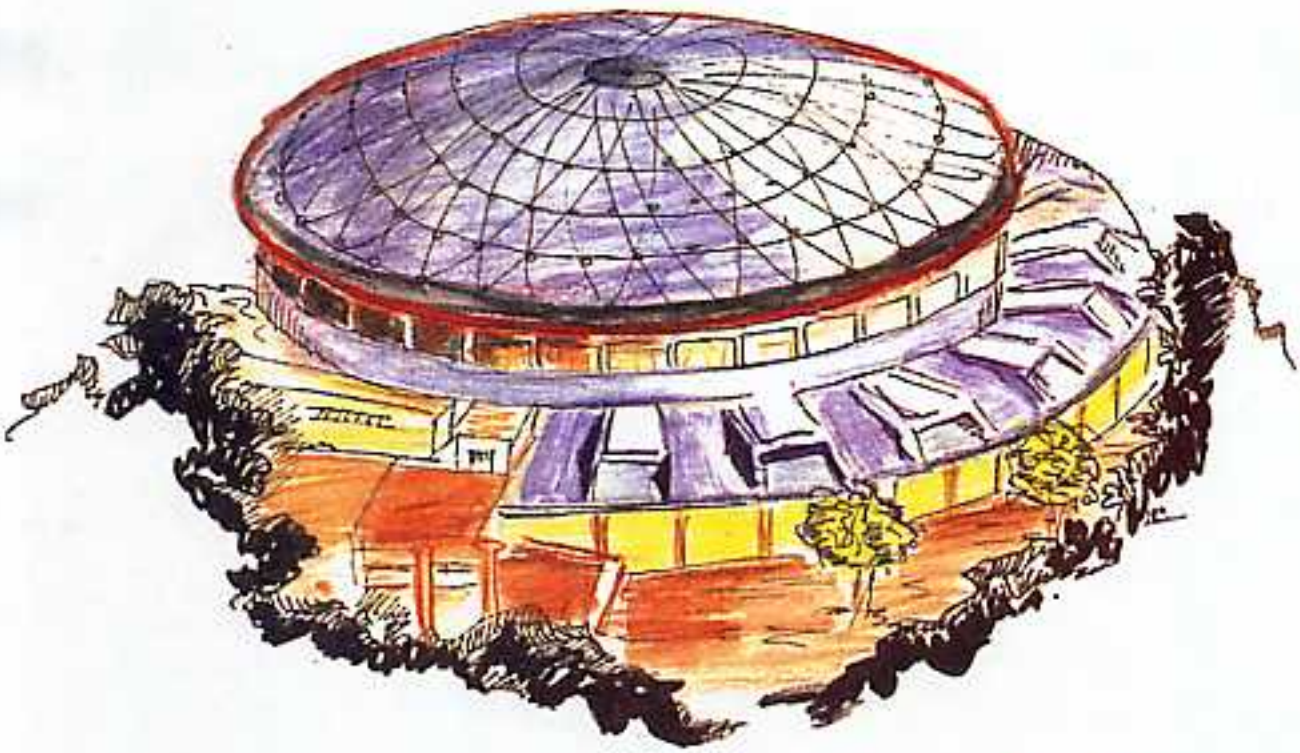

Servizio Documentazione
dei Laboratori Nazionali di Frascati
P.O. Box, 13 - 00044 Frascati (Italy)

INFN - Laboratori Nazionali di Frascati
Servizio Documentazione

LNF-92/107 (P)
16 Dicembre 1992

# COMMISSIONING AND PERFORMANCE OF A LOW EMITTANCE, LONG PULSE ELECTRON GUN FOR THE SC LINAC LISA

M. Castellano, S. Kulinski, P. Patteri, F. Tazzioli, M. Vescovi
INFN – Laboratori Nazionali di Frascati, P.O.Box 13, I–00044 Frascati (Rome) Italy

N. Cavallo, F. Cevenini
INFN – Sezione di Napoli and Dipartimento di Fisica, Università di Napoli, Padiglione 20, Mostra d'Oltremare, I–80125 Napoli, Italy

## ABSTRACT

A 25 MeV superconducting linear accelerator (LISA) is in construction in the Frascati INFN Laboratories. Here we describe the design and measured performances of the electron gun, that can deliver 200 mA dc at 100 kV with normalized emittance of less than 10–5 m rad.

## 1 – INTRODUCTION

The ARES project funded by the Italian Agency INFN, and based mainly in the Frascati Laboratory, aims at developing high gradient superconducting cavities and low emittance, high brightness, electron beams required for future high energy Linear Colliders.

In the framework of this project, the construction of the small superconducting linear accelerator LISA has the purpose to develop the know–how on superconducting cavities and on related technologies, together with the capability of producing and transporting high quality electron beams.

The first application of LISA will be the realization of an infrared Free Electron Laser, both a suitable diagnostic tool for beam quality and a versatile device for molecular and solid state physics research. LISA has been extensively described in previous papers [1]. Here we briefly recall the main design parameters, with reference to Fig. 1, where a general layout is shown.

The electrons are produced by a Pierce type, 100 kV thermionic gun, in a triode configuration, with a nominal DC current of 200 mA. Although the accelerator can in principle work in the CW mode, radiation safety regulations limit the average beam power to 1 kW. To maintain the high peak current required by the FEL application, we therefore have to pulse the gun with a duty cycle of 2 %.

Two choppers, operating at 50 and 500 MHz, provide a train of 40 pC microbunches spaced by 20 ns, reducing the average current in the macropulse to a mean value of 2 mA.

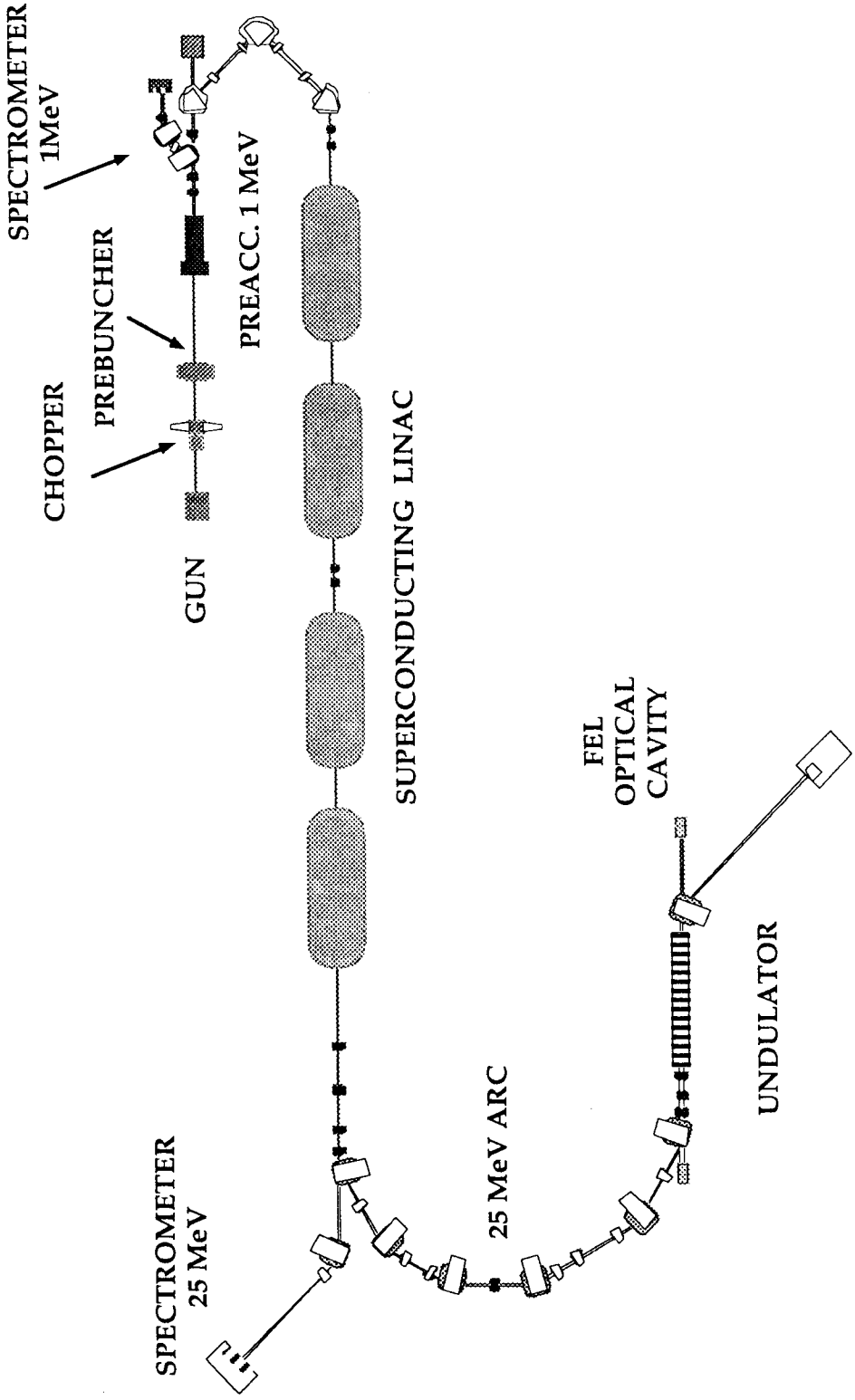


***FIG. 1*** *– General layout of LISA accelerator and related FEL experiment.*

A 10 kV buncher cavity at 500 MHz, followed by a drift space, compresses the bunches to 8 ps at the entrance of a 1 MeV, 2500 MHz, β–graded preaccelerator section, giving a final peak current of 5 A.

Since FEL operation requires high peak current and low emittance, much care has to be taken to preserve the beam quality along the transport line.

The final beam emittance cannot be better than that delivered by the gun, therefore a preliminary measurement of its dependence on the gun parameters is of crucial interest. Moreover, being the first gun of its kind designed in house and built to our own specification, a complete characterization, including all ancillary equipment, was necessary.

## 2 – THE GUN

### 2.1 – Design parameters

The basic requirements for the LISA gun are summarized in Table I.

**Table I – Required parameters for the LISA gun.**

| | |
|---|---|
| Current (DC) | I = 0.2 A |
| Energy | W = 100 keV |
| Energy dispersion | $\Delta W/W = 10^{-3}$ |
| Emittance (invariant) | $\varepsilon \leq \pi\ 10^{-5}$ m rad |

Since we are limited only in mean beam power, a pulse length variable up to DC was specified in order to meet the requirements of an almost CW FEL.

A modified Pierce geometry has been optimized at LNF. The electron optics was modeled using Hermannsfeldt's code E–GUN [2], which is the most used code in guns' design, notwithstanding its limitations particularly evident in our case (see par. 5). An example of beam dynamics inside the gun is shown in Figure 2. The results of this study were reported in [3], and used to specify the geometrical parameters listed in Table II. The gun has been constructed by PROEL (Firenze).

**Table II. – Geometrical parameters of the LISA gun.**

| | |
|---|---|
| Type | Pierce, triode |
| Cathode radius | $R_k$ = 40 mm |
| Radius of focussing electrode | $R_{fe}$ = 15 mm |
| Curvature radius of focussing electrode | $R_{fe}$ = 3 mm |
| Length of focussing electrode | $L_{fe}$ = 18 mm |
| Anode hole diameter | $\Phi_a$ = 8 mm |
| Anode curvature radius | $R_a$ = 2 mm |
| Cathode to anode distance | $d_{ca}$ = 32 mm |

The high voltage power supply has been designed for 20 kW DC, giving 200 mA at 100 kV, in order to ensure an ample range of pulse lengths. It is voltage regulated in the range 10 – 100 kV, with a maximum ripple of ± 100 V.

The grid pulse generator with 100 kV insulation gives a maximum pulse amplitude of ± 500 V with ripple of ≤ 0.1 %. Control and monitoring signals are transmitted through fiber optics with a passband of 10 kHz and linearity better than 1%.

All gun parameters can be remotely controlled, in particular the grid pulse length can be varied from 0.2 ms up to DC. The gun power supply was constructed by EL–EN (Firenze).

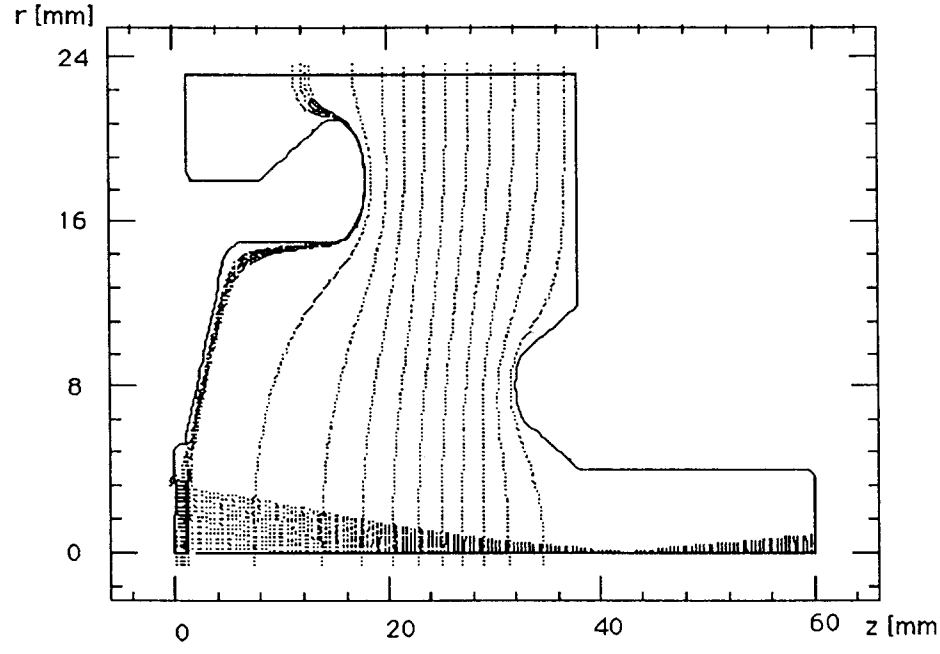


*FIG. 2 – Electron trajectories and equipotential lines. Va=100 kV, Vg=445 V.*

2.2 – Computed performance

The perveance G of the triode is defined by

$$I = G\ Veq^{3/2}$$

where I is the anode current and $V_{eq}$ is the equivalent potential on the grid surface, given by

$$Veq = ( Vg + Va/\mu ) \qquad (2.1)$$

with Vg the grid potential, Va the anode voltage and μ the triode amplification factor.

More precisely

$$Veq = (Vg + Va/\mu)/(1 + 1/\mu + (4/3\mu)(d_{ga}/d_{cg})) \qquad (2.2)$$

where $d_{ga}$ is the grid–anode distance and $d_{cg}$ the cathode–grid one.

The amplification factor μ can be calculated [4] to be

$$\mu = ( 2\pi(d_{ga}/a) - \ln(\cosh(\pi S)))/\ln(\coth(\pi S))$$

with '$r_g$' the grid wire radius, 'a' the spacing between parallel wires, and $S = 2r_g/a$ the screening fraction.

This formula is accurate to within few percent up to screening fractions of ≈ 0.2. Taking our values: $d_{ga}$ = 31 mm, a = 1 mm, $r_g$ = 0.1 mm we get S = 0.2 and $\mu$ = 332.

The calculation of the perveance is more difficult since other factors, beside the geometry, shuch as homogeneity of cathode surface emissivity, cathode temperature and electric field distribution on the grid surface should be taken into account. Since the distance $d_{cg}$ is short, we can use the well known formula for the planar diode in the space charge controlled regime to evaluate the current density distribution

$$J = 2.3\ 10^{-6}\ V_{eq}^{1.5}/d^2 \quad (A/cm^2)$$

The total emitted current is then $I = \pi\ R_c^2\ J$ , where Rc is the cathode radius and d the cathode to anode distance.

Taking $d = d_{cg}$ = 1 mm, $R_c$ = 3.2 mm, we obtain G = 6.26 $10^{-5}$, using equation (2.2).

## 3 – THE EXPERIMENTAL SET–UP

### 3.1 – General Description

The first part of the channel assembled for the gun test was the same as that installed on the accelerator: starting from the gun output flange, it consists of a short 40 mm diameter stainless steel pipe with extensions for roughing and ion pumps, closed by an all metal valve. The pipe prolongs for about 20 cm after the valve, allowing the installation of steering coils, and is then interrupted by a ceramic insertion around which a toroidal beam current monitor is mounted.

A shielded solenoidal lens is positioned right next to the gun. The 40 mm long coil has 40 turns; the iron shield has a 20 mm gap and is directly fastened to the pipe, with a corresponding internal diameter of 42 mm.

The following part of the channel has been specifically designed for this test and consists mainly of a chamber containing a 45° tilted fluorescent screen viewed by a CCD TV camera through an optical window. The screen can be removed from the beam line allowing direct observation of the cathode through an on–axis window. The chamber carries extensions to connect ion and roughing vacuum pumps.

The screen is a 5 cm side square; its distance from the solenoid lens has been chosen so that the image of the beam waist at the gun exit is magnified by a factor ten at the target. The power density on target is thus reduced and the resolution of the beam spot measurement increased.

### 3.2 – Data Acquisition System

The fluorescent screen is viewed by a high linearity CCD TV camera with a resolution of 512x512 pixels. The output video signal of the camera is sent to an image grabber processor ( MVP–VME Matrox Vision Processor), a three unit plug in a standard VME crate. The processor can handle up to four different TV cameras, and is provided with a powerful firmware for image analysis.

The VME crate is interfaced to a Macintosh II personal computer which is used for data storage, simple on–line interactive analysis and final off–line data reconstruction.

The software for data acquisition and analysis is written in RTF (Real Time Fortran) [5].

The whole system is compatible with the final Control System of the accelerator [6], allowing an easy insertion of the measurerement among the tasks routinely available to the operator in a fully automatized procedure.

3.3 – Calibrations and First Beam Test

The toroidal current monitor sensitivity (100 mV/A) is calibrated by means of a known current pulse through an auxiliary winding. A second current monitor, calibrated in the same way, is installed around the high voltage power supply cable.

The cathode temperature versus filament current is determined by looking directly at the cathode surface with a pyrometer through the on axis windows. The standard procedure to activate the cathode is followed, fixing the final temperature at 1020 °C.

The grid pulse is driven by a pulse generator through a remote external input. In this way one has complete control of the bias level, pulse length, amplitude and frequency. The actual values of bias and pulse amplitude at the grid are monitored by means of the echoed pulse available on the remote control panel of the gun power supply .

The first beam tests were performed using an aluminium fluorescent screen with a thin phosphor coating, providing good optical efficiency also at very low electron current and energy. The grid pulse was kept as short as possible (300 μs), consistent with the overall system bandwidth, and the initial repetition rate was 1 Hz.

In spite of these precautions, after few minutes the screen surface was severely damaged, the pressure rose to $10^{-7}$ Torr and the cathode emissivity decreased sharply.

This showed that evaporable material cannot be used on the screen, because it cannot sustain the long electron pulse, even at low duty cycle.

The cathode emissivity was partially recovered by a new activating procedure, but, as a consequence of cathode poisoning, the emissivity versus temperature curve now showed a maximum at 880 °C, decreasing rapidly at higher temperature. A current of 250 mA with an anode voltage of 90 kV was obtained in this way, 300 mA could be reached by heating the cathode at 1040 °C for few minutes and then going back to 880 °C. At the moment no final explanation for this effect has been found.

A new screen (chromium doped aluminium oxide) was installed bearing a set of reference points, spaced one centimetre on the perimeter of a square of 2 cm side, used to calibrate the TV picture.

This kind of screen sustained the beam power well, at least for short pulses (few hundred microseconds) and low duty cycle (1 Hz), and the vacuum showed little deterioration due to beam induced desorbtion; there was nevertheless clear evidence (one screen was broken) of thermal stresses for long pulses (> 1ms) and tightly focussed beams.

In the progress of work, we also tested other kinds of screens. In particular, aluminium foil with a thin layer of glued fine aluminium oxide powder and aluminium foil with 30 μm surface anodisation proved to behave quite well, the latter showing a better surface uniformity.

After having solved minor problems caused by electromagnetic transients due to the gun conditioning, we were left with a high instability in the beam dynamics due to the

charging of the ceramic insertion by dispersed electrons. A conductive shield inside the insertion preventing the electrons from directly hitting the ceramic definitively solved the problem.

With a stable beam, the current measured by the monitor on the power supply cable was equal to that measured by the monitor on the beam pipe for a wide range of magnetic lens strengths. A large beam divergence at the gun exit was indicated by the strong focussing needed to prevent beam losses before the current monitor.

## 4 – EXPERIMENTAL RESULTS

### 4.1 – Gun Characteristics

The behaviour of beam current as a function of the grid potential for different values of the cathode voltage is shown in Fig. 3.

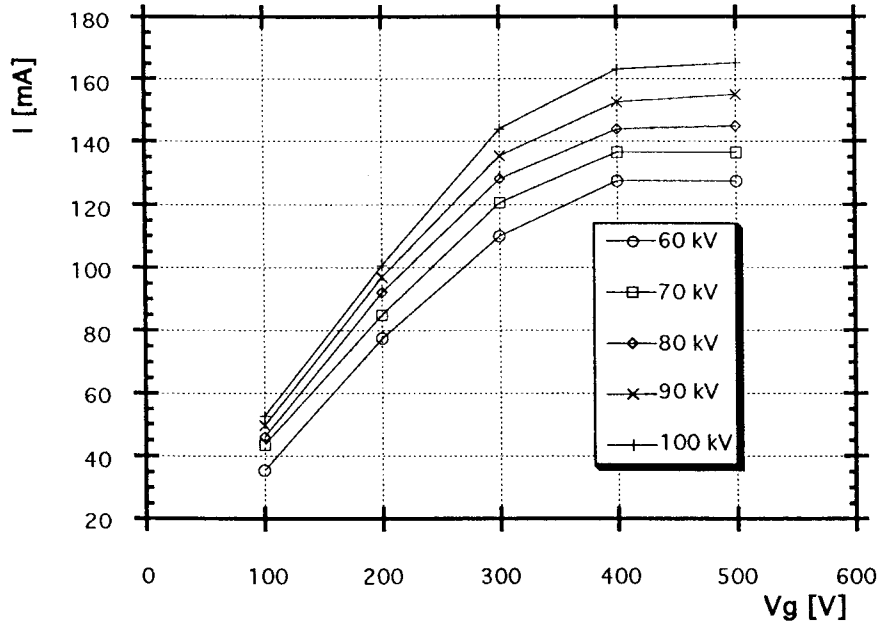


*FIG. 3 – Gun current versus grid potential for different values of anode voltage.*

The gun current versus cathode voltages at the fixed grid potential of 500 Volts is shown in Fig. 4. The continuous curve is a fitted function of the kind

$$I = G\left[500 + \frac{V_a}{\mu}\right]^q$$

giving $G = 6\ 10^{-6}$, $\mu = 319$ and $q = 1.52$. The exponent is very close to the theoretical value of 1.5, and if we fix it to this value, we obtain $G = 7\ 10^{-6}$, $\mu = 311$.

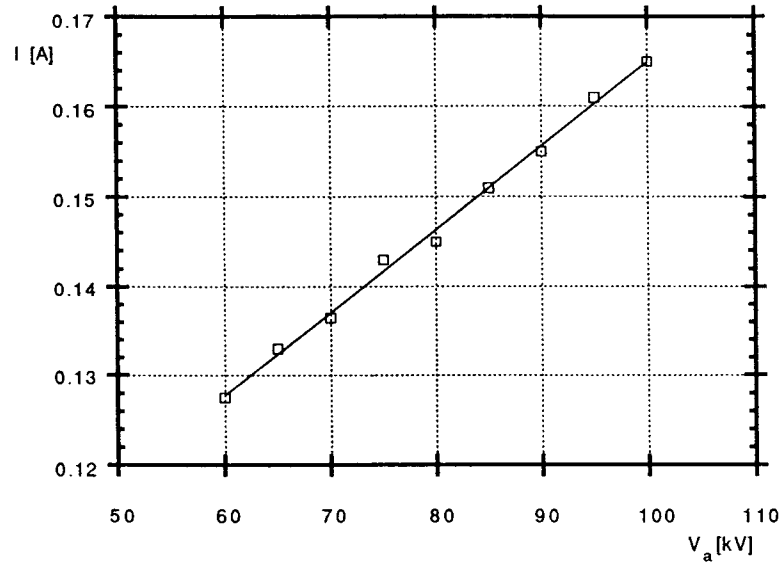


***FIG . 4*** *– Gun current versus anode voltage at 500 V fixed grid potential.*

4.2 – Transverse emittance measurement

4.2.1 – Principles of measurements

The simple set up of the gun test line can be used to measure the transverse emittance by the fixed screen, variable focussing method.

In fact the evolution of the Twiss parameters from an arbitrary starting point to the target is given by the well known expression

$$\begin{bmatrix} \beta \\ \alpha \\ \gamma \end{bmatrix} = \begin{bmatrix} m_{11}^2 & -2m_{11}m_{12} & m_{12}^2 \\ -m_{11}m_{21} & m_{11}m_{22}+m_{12}m_{21} & -m_{12}m_{22} \\ m_{21}^2 & -2m_{21}m_{22} & m_{22}^2 \end{bmatrix} \begin{bmatrix} \beta_o \\ \alpha_o \\ \gamma_o \end{bmatrix} \qquad (4.1)$$

$\beta_o$, $\alpha_o$, $\gamma_o$ being the Twiss parameter initial values and $m_{ij}$ the elements of the trasport matrix between the two points, that depend only on the optical elements strength and position. It follows that the spot dimension at the target, $\sigma$, is given by

$$\varepsilon\,\beta \equiv \sigma^2 = m_{11}^2\,(\varepsilon\,\beta_o) - 2m_{11}m_{12}\,(\varepsilon\,\alpha_o) + m_{12}^2\,(\varepsilon\,\gamma_o) \qquad (4.2)$$

and is a function of only three out of the four unknowns, $\varepsilon$, $\beta$, $\gamma$, $\alpha$, since the Twiss parameters are coupled by the relation

$$\beta\gamma - \alpha^2 = 1 \qquad (4.3)$$

In principle just three measurements of the spot size at three different settings of the transport matrix would allow solving a linear system in the unknowns $\varepsilon\beta$, $\varepsilon\alpha$, $\varepsilon\gamma$. $\varepsilon$ so that the Twiss parameters can then be determined from equation (4.3).

However, the solution of the linear system is rather sensitive to experimental errors in the spot size measurement, so that this straightforward procedure is inadequate.

A frequently used procedure to overcome this difficulty consists in taking more than three measurements and to determine the unknown variables that minimize the function

$$\mathbf{f} = \sum_i \left(\sigma^2 - \left(\mathbf{m}_{11}^2(\varepsilon\beta_o) - 2\mathbf{m}_{11}\mathbf{m}_{12}(\varepsilon\alpha_o) + \mathbf{m}_{12}^2(\varepsilon\gamma_o)\right)\right)^2 \qquad (4.4)$$

In our case, the length of the solenoid being short compared to the lengths of the preceding and following free drift spaces, the thin lens approximation can be used for the solenoid transport matrix. In this approximation eq. 4.2 produces a quadratic dependence of $\sigma^2$ on the solenoid current $I_s^2$. From the polynomial coefficients of a best fit to the experimental data one can then evaluate the Twiss parameters and the emittance.

Note that the method is only accurate enough if space charge forces along the drift from the lens to the screen do not substantially modify the emittance value.

To verify whether this condition is satisfied by our test set–up, we have extended the simulation with the E–GUN code to include the iron shielded solenoid and the following drift space to the screen (see e.g. Fig. 5); the simulation shows that downstream from the solenoid no substantial emittance degradation occurs unless the beam is brought to a (small) focus in between the solenoid and the screen, a condition that has therefore been carefully avoided.

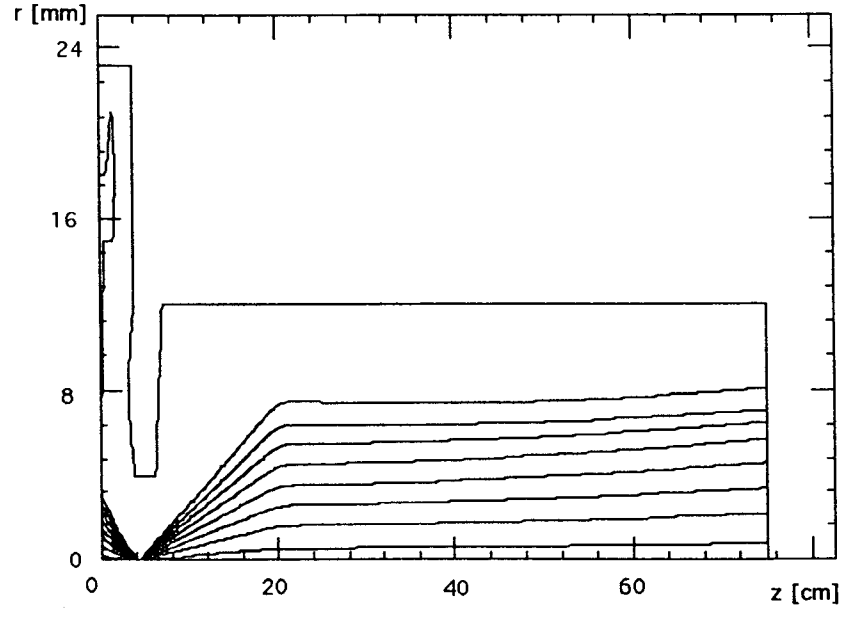


*FIG. 5 – E–GUN simulation of the beam behaviour up to the screen with Va=100 kV, Vg=350 V and I=200 mA. A shielded coil is placed at z=20 cm with NI=1220 amperturns corrisponding to Bm=426 Gs.*

4.2.2 – Experimental results

Data were taken for different settings of both the accelerating voltage and the beam current. Because of the peculiar behaviour of the test cathode its temperature had to be kept constant at the value of maximum emissivity and the gun current could only be varied by acting on the grid voltage; consequently, the emittance could not be optimized for all operating condition.

For the reason described above, measurements of spot size versus solenoid current were only taken under conditions such that the beam was not brought to a focus upstream from the screen.

A 3D plot of the beam intensity, an example of which is presented in Fig. 6, shows rather sharp edges with a small diffuse halo. Because in the final injector assembly the halo was expected to be removed by a collimator, the rms beam spot size has been evaluated using the image fraction delimited by an ellipse containing 90 % of the total picture intensity. This cut gives a more realistic value of the size of the transportable beam. It also provides a better fit due to a smoother behaviour of spot size versus lens strength.

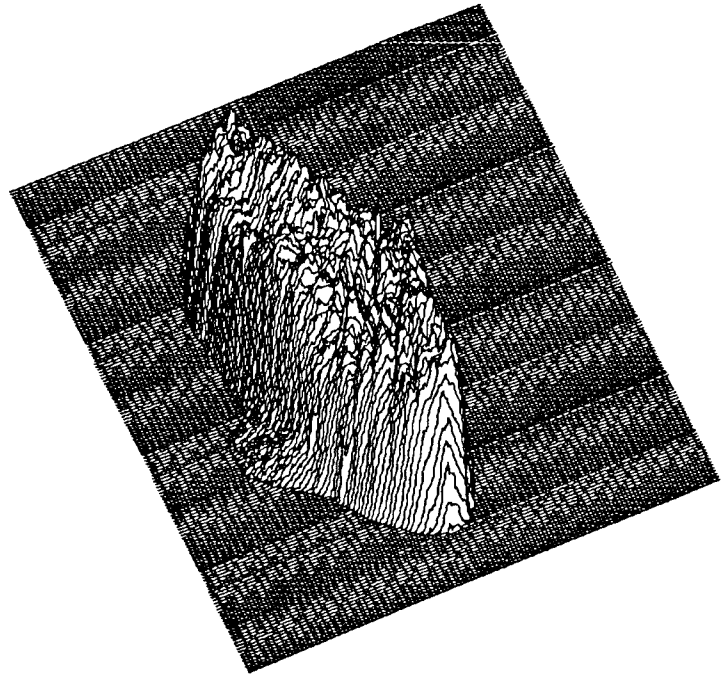

*FIG. 6 – 3D image of the electron beam as seen by the camera without normalization of x and y dimensions.*

Systematic measurements of screen linearity as a function of peak current and integrated charge have been performed at SLAC [7] on the same kind of screen, showing that the screen response is linear over several orders of magnitude. Furhtermore, the measured constance of the integrated picture intensity as a function of the lens strength, over rms spot sizes ranging from 5 to 2 mm, showed that there was no saturation up to the maximum tested current.

Repeated measurements of the spot size and of its centre position under costant experimental conditions give rms errors of 1 % and ± 50 μm respectively, confirming the stability of the whole system and in particular of the gun power supply.

The emittance measurement results are summarized in Figure 7, showing the rms emittance behaviour versus beam current at different accelerating voltage values.

The statistical error on individual emittancemeasurements is derived from the errors on the polinomial fit coefficients and found to be to be in the range from of 6% to 10%.

As said above, the data also allow to determine the Twiss coefficients at the solenoid entrance. It is thus possible to follow the beam back through the drift space to the waist produced by the gun electrodes.

The results obtained by this procedure - for an accelerating voltage of 90 kV - are shown in figure 8: the computed distance d of the waist from the solenoid and the waist radius σ are plotted as functions of beam current.

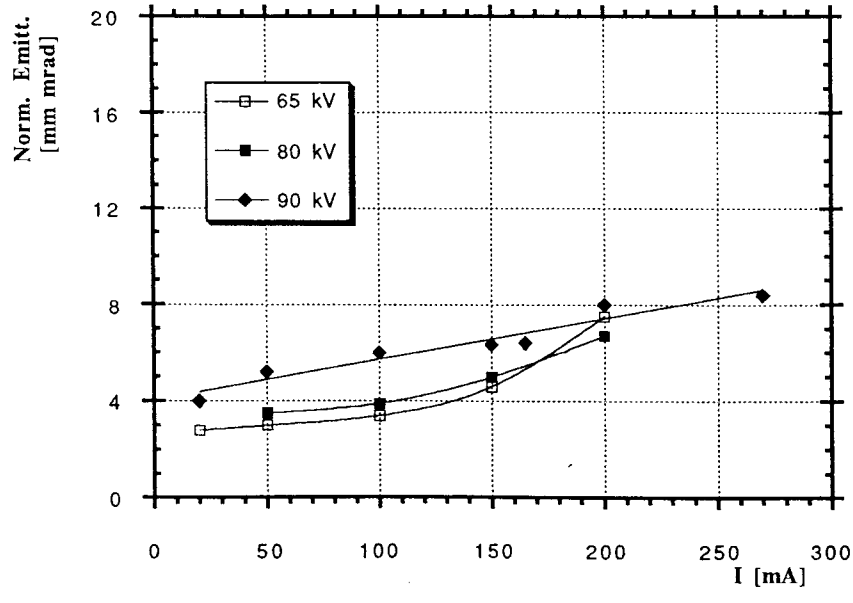


*FIG. 7 – Normalized rms emittance* $\varepsilon = \beta\gamma\sqrt{\langle x\rangle^2\langle x'\rangle^2 - \langle xx'\rangle^2}$ *as a function of gun current for different values of accelerating voltage.*

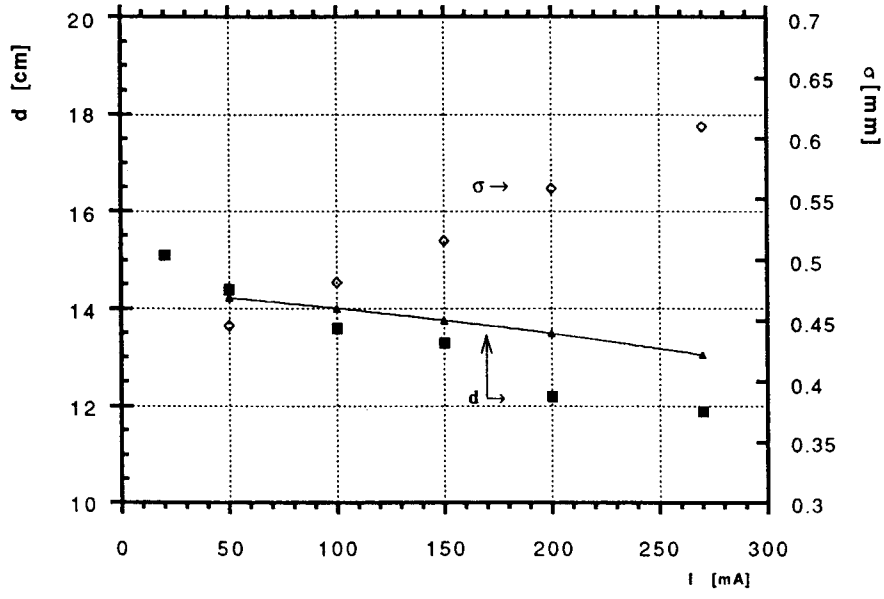


*FIG. 8 – Beam waist radius and distance from the solenoid as a function of the current at 90 kV. The continous line is the result of computing dwith E–Gun .*

## 5 – CONCLUSIONS

The outcome of the tests proves that gun and power supply design specifications have been met, except for the limitation on the maximum achievable current ascribed to the peculiar behavior of the cathode emissivity; the latter effect was was conjectured to be due to poisoning of the cathode as a consequence of the accident with the phosphorized target, and in fact was never since observed on clean cathodes.

Comparing experimental results with theoretical calculations we find good agreement on the triode amplification factor, while a disagreement by one order of magnitude exists on the perveance as a consequence of the cathode impaired emissivity.

For comparison with the experimental results, Hermannsfeldt's E–GUN code was run for a number of cases in the range of gun voltages and current intensities covered by the measurements: the simulations confirmed the inadequacy of the code, already remarked upon above, for describing the evolution of the electron beam delivered by a gun such as ours. The inadequacy originates from a number of known limitations inherent in the code, whose results must therefore be taken with care.

The main problems arise in the evaluation of beam emittance for two separate reasons:

a) the lowest possible theoretical emittance of a thermionic gun is usually accepted to be determined by thermal agitation and to be given by

$$\varepsilon_{therm} = 2R_c\sqrt{(kT / m_o c^2)} \qquad (4.5)$$

where $R_c$ is the cathode radius, T is the temperature and $m_0c^2$ the electron rest energy. The way in which the code can account for this lower emittance limit, due to the fact that the electrons emitted from the cathode have a transverse velocity distribution depending on the cathode temperature, is rather crude: current rays are divided into at most 5 different groups having different initial transverse velocities. The main effect of the small number of different rays over which the current can be distributed is to produce large fluctuations in the final emittance value as function of total current, as can be seen from the computed data of figure 9 ;

b) furthermore, for triode guns using a grid to control the emitted current, E–Gun treats the grid as a constant potential surface. But the actual metallic wire mesh produces a much more complicated field distribution that can considerably disturb the electron trajectories. In fact, recent independent measurements comparing a a diode to a triode gun [8] show that the measured diode emittance is only slightly larger than $\varepsilon_{therm}$ while the emittance of the gridded gun turns out to be 6–7 times larger. Note that this effect was anticipated, and an attempt was made to partly remedy to the emittance deterioration by designing for a value lower than specified.

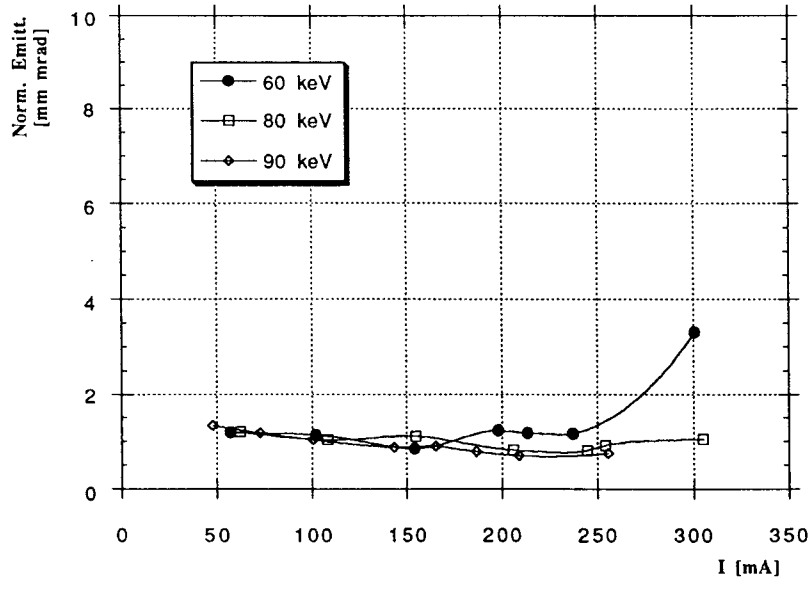


*FIG. 9 – Normalized rms emittance ($\varepsilon = \beta\gamma\sqrt{<x>^2<x'>^2-<xx'>^2}$) obtained by the E–Gun code with cathode thermal emittance corrisponding to a temperature of 1020 °C.*

Our final measured values are a factor of ≈ 4 larger than those predicted by the simulations, in qualitative agreement with the results of reference [8].

The measured data also exibit the expected emittance blow up with increasing current

at all energies, the effect beeing larger the lower the energy; however the low current behaviour of the absolute value of emittance as a function of energy, evidenced in figure 8, showing a slight decrease in emittance with decreasing energy are in disagreement with the expectations and not well understood.

On the other hand, although the measured emittance and beam waist size differ considerably from the computed ones, the waist distance from the cathode is in reasonable agreement with the computations, as shown by Fig. 8.

## ACKNOWLEDGMENTS

Dr. A. Ghigo helped us during the first stages of the work. The staff of the Operation Service of the LNF Accelerator Division, in particular S. Pella, G. Piermarini and R. Valtriani, provided continuous and competent technical support.

## REFERENCES

[1] A. Aragona et al. –The Linear Superconducting Accelerator Project LISA, Proceedings of the European Particle Accelerator Conference–Roma 1988, 52, (1989).
M. Castellano – An Infrared Free Electron Laser on the Superconducting Linac LISA – LNF–88/04(R) (1988).
F. Tazzioli et al. – Status of the LISA Superconducting Linac Project, Proceedings of "1991 Particle Accelerator Conference", San Francisco IEEE 91CH3037–7, 2971 (1992).

[2] W.B. Hermannsfeldt – Electron Trajectory Program – SLAC Report 226.

[3] S. Kulinski and M. Vescovi – A Gun for LISA – LNF–87/98(R) (1987).

[4] K.R. Spangenberg – Fundamentals of Electron Devices – McGrow–Hill, New York 1957.

[5] H. von der Schmitt – RTF/68K, Real–Time FORTRAN–77 for 68K Processors – Physikalisches Institut Universitat Heidelberg and CERN UA1 – March 9, (1988)

[6] M. Castellano et al– Computer Control and Diagnostic Equipment for the LISA Project – Proceedings of the 2nd European Particle Accelerator Conference – Nice. Editions Frontières 866 (1990).

[7] J.T. Seeman, V. Luth, M. Ross and J. Sheppard – Beam Test of Phosphorescent screen – Single Pass Collider Memo CN–290 – SLAC 1985.

[8] B. Strongin and A. Salop – Emittance Determination of Electron Guns by Analysis of Beam Profile Measurements. – Proc. 1990 Linear Acc. Conf. – Albuquerque – New Mex. Los Alamos LA–12004–C (1991).